Journal of Seismology **1**: 3–14, 1997.

The February 1996 earthquake sequence in the eastern Pyrenees: first results

A. Rigo[1], H. Pauchet[1], A. Souriau[1], A. Grésillaud[1], M. Nicolas[2], C. Olivera[3] & S. Figueras[3]
[1] *Observatoire Midi-Pyrénées, GRGS – CNRS UMR 5562, 14 Ave. E. Belin, 31400 Toulouse, France*
[2] *Laboratoire de Détection et de Géophysique, CEA, B.P. 12, 91680 Bruyères-le-Châtel, France*
[3] *Institut Cartogràfic de Catalunya, Servei Geològic de Catalunya, Parc de Montjuïc, 08038 Barcelona, Spain*

Received 16 October 1996; accepted in revised form 28 April 1997

Abstract

An earthquake with local magnitude (M_L) 5.2 occurred 18 February 1996 in the eastern Pyrenees (France) near the town of Saint-Paul de Fenouillet. This event is the first of this magnitude in France to be well recorded instrumentally. Less than 24 hours after the main shock, we installed a temporary network of 30 seismological stations in the epicentral area to record the aftershock sequence. In this paper, we analyse the main shock and present the 37 largest aftershocks ($1.8 \leq M_l \leq 3.4$) in the two months following the main shock. These events are located using data from the permanent Pyrenean seismological network and the temporary network when available. We also determined eight fault plane solutions using the P-wave first motions. The main shock and the aftershocks are located inside the small Agly massif. This Hercynian structure is located some 8 km north of the North Pyrenean Fault, which is usually considered to be the suture between the Iberian and Eurasian plates. The mechanism of the main shock is a left-lateral strike-slip on an E–W trending fault. The fault plane solutions of the aftershocks are mostly E–W striking reverse faults, in agreement with the general north-south shortening of the Pyrenees. The aftershocks located down to 11 km depth, indicating that the Agly massif is deeply fractured. The main interpretations of these results are: (i) the main shock involved an E–W trending fault inside the highly fractured Agly massif, relaying the North Pyrenean Fault which had, at least in the last 35 years, a poor seismic activity along this segment; (ii) the Saint-Paul de Fenouillet syncline to the north and the North Pyrenean Fault to the south delimit a $\sim$ 15 km wide senestral shear zone. Such a structure is also suggested by the highly fractured pattern of the Agly massif and by small en echelon faults and secondary folds in the Saint-Paul de Fenouillet syncline; (iii) we suggest that the North Pyrenean Frontal Thrust, located less than 10 km north of the Agly massif, has a ramp geometry at depth below the Agly massif.

Introduction

On February 18, 1996, a local magnitude $M_L = 5.2$ earthquake occurred in the eastern Pyrenees near the town of Saint-Paul de Fenouillet (Figure 1). This event, the strongest in the Pyrenees range since the Arette earthquake ($M = 5.7$) in 1967 and the Arudy earthquake ($m_b = 5.1$) in 1980 in the western Pyrenees (Gagnepain-Beyneix et al., 1982), is the first of its size in France to be recorded by a large number of permanent instruments. It was followed by hundreds of aftershocks, twelve of which had duration magnitude M_l above 3.0. Shortly after the main shock, French and Spanish institutions deployed temporary seismological networks. These instruments furnished a large number of data, which we analyse in the context of the Pyrenean tectonics.

The Pyrenean range is the result of the continental collision between the Iberian and Eurasian plates. This collision took place after an extensive episode related to the opening of the Bay of Biscay during the lower Cretaceous (80–120 Ma). Several scenarios have been proposed for this opening, involving either a large anticlockwise rotation (35 °) of Iberia with respect to Eurasia, or a scissors-opening of the Bay of Biscay (see Choukroune, 1992, for a review). The different models all involve more extension in the western part of the Pyrenees than in the eastern part. The extensive episode was followed by the north-south convergence of the Iberian and Eurasian plates beginning in the upper Cre-

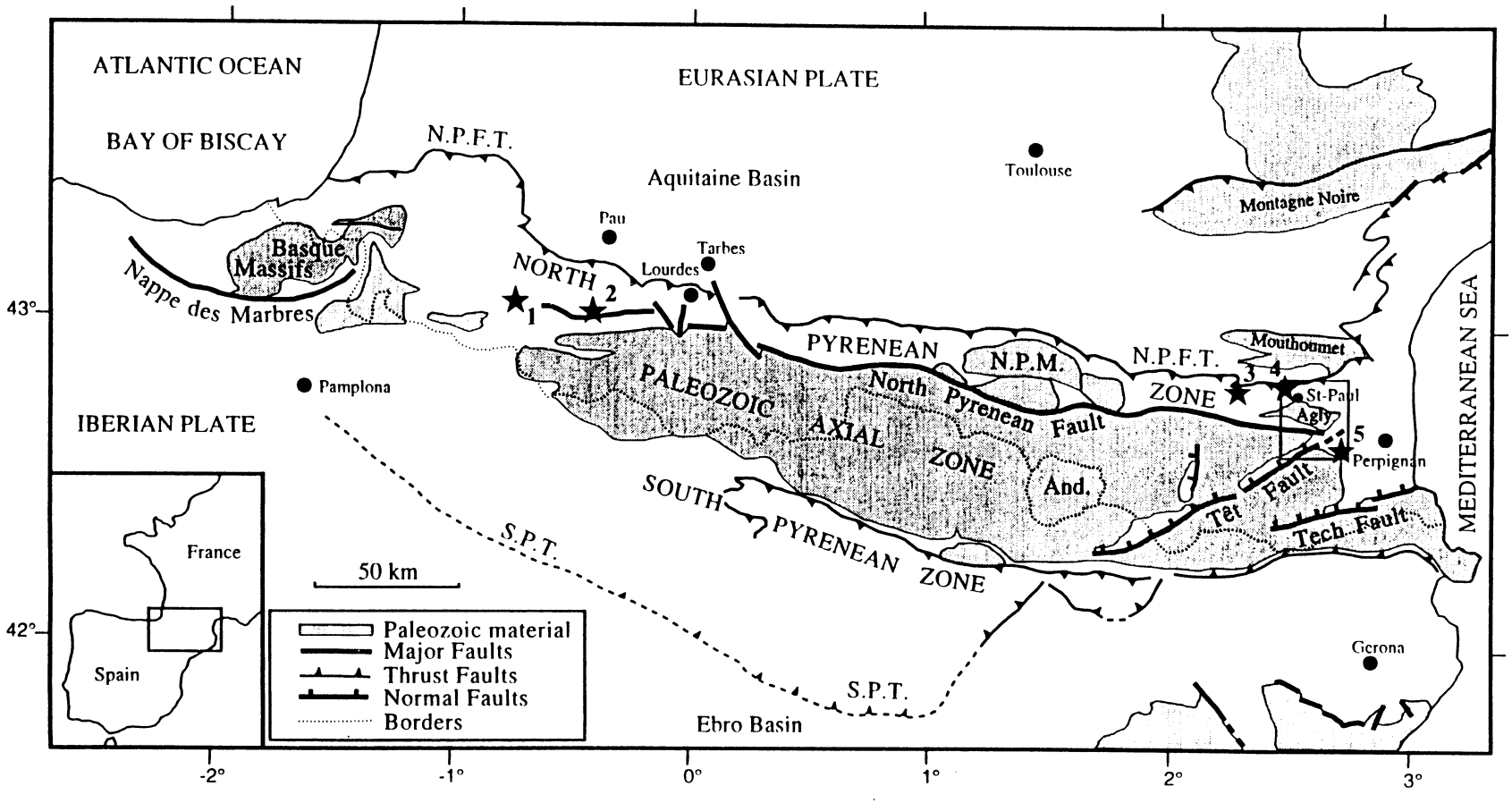

Figure 1. Tectonic map of the Pyrenees redrawn from Souriau and Granet (1995) and Briais et al. (1990). N.P.M.: North Pyrenean Massifs; N.P.F.T.: North Pyrenean Frontal Thrust; S.P.T.: South Pyrenean Thrust; And.: Andorra. The box including the Agly massif and the town of Saint-Paul de Fenouillet in the eastern Pyrenees corresponds to Figures 3 and 4. Stars show important earthquakes 1: Arette earthquake, $M = 5.7$, 1967 (Gagnepain-Beyneix, 1987); 2: Arudy earthquake, $m_b = 5.1$, February 29, 1980 (Gagnepain-Beyneix et al., 1982); 3: The November 28, 1920 earthquake, I = V–VI; 4: The September 23, 1922 earthquake, I = VI–VII; 5: The December 28, 1922 earthquake, I = VI (Cadiot et al., 1979; Lambert and Levret-Albaret, 1996).

taceous (65 Ma), with more or less senestral motion in the axial zone of the range according to the different models (Choukroune, 1992). The resulting north-south shortening continues to the present day and amounts to about 50–150 km in the central and eastern Pyrenees (Roure et al., 1989). It has been accommodated by a subduction of the Iberian lower crustal material beneath the Eurasian crust (Engeser and Schwentke, 1986; ECORS Pyrenees Team, 1988; Choukroune and ECORS Team, 1989; Daignières et al., 1989; Torné et al., 1989; Mattauer, 1990), which is well observed from tomographic models in the central and eastern parts of the range (Souriau and Granet, 1995).

The overall east-west structure of the Pyrenean range (Figure 1) can be described, from north to south, as follows:

(i) the North-Pyrenean Zone (NPZ): it is mainly composed of highly deformed Mesozoic flysch deposits (Puigdefabregas and Souquet, 1986). It rides northward over the Aquitaine molasse basin along the North Pyrenean Frontal Thrust (N.P.F.T. in Figure 1). The North Pyrenean Zone includes a few Palaeozoic outcrops, including the North Pyrenean Massifs (N.P.M. in Figure 1) in the central part of the range, and the small Agly massif to the east. The North Pyrenean Massifs originated as an allochton unit, from the Palaeozoic Axial Zone (Goldberg et al., 1986; Souquet and Peybernès, 1987).

(ii) The Palaeozoic Axial Zone: it is the central unit, and includes the highest summits of the range. It is composed of Hercynian structures reactivated during the Alpine orogeny.

(iii) The South Pyrenean Zone: it is composed of Mesozoic and Cenozoic sediments, which slid southward down from the Axial Massifs when they rose.

The limit between the North Pyrenean Zone and the Palaeozoic Axial Zone is a major tectonic suture called the North Pyrenean Fault (Figure 1), which is usually considered to be the boundary between the Eurasian and Iberian plates. This fault, which runs east-west all along the mountain belt, coincides with an important vertical offset of the Moho, with a thicker crust beneath the Iberian side. The Moho offset reaches 15 km in the central part of the range (Hirn et al., 1980; Gallart et al., 1981; Daignières et al., 1982; Choukroune and ECORS Team, 1989), but it does not exceed 5 km in the eastern part (Gallart et al., 1980, 1982). The North Pyrenean Fault is characterised by highly strained metamorphic rocks formed at high temperature and low pressure during the extensive episode. This episode emplaced lherzolite massifs all along the North Pyrenean Fault in the sediments of the North Pyrenean Zone (Vielzeuf and Kornprobst, 1984; Bouhallier et al., 1991; Paquet and Mansy, 1991). The Arette and Arudy earthquakes took place on the North Pyrenean Fault in the western Pyrenees (Gagnepain-Beyneix et al., 1982; Gagnepain-Beyneix, 1987) (Figure 1).

This overall structure is complicated in the eastern part of the range by structures resulting from a phase of extension which began in the late Eocene time. This last phase corresponds to the opening of the Gulf of Lion and the eastward migration of the Corso-Sardinian block (Rehaut et al., 1984). Consequently, several major normal faults with roughly NE–SW orientation are present at the eastern end of the Pyrenean range, in the Gulf of Lion and along the Iberian Mediterranean margin. These major normal faults appear to be active through the present day from morphological criteria (Briais et al., 1990), although small reverse quaternary faults have been observed in the same area (Philip et al., 1992).

The 1996 earthquake occurred near the town of Saint-Paul de Fenouillet, in the North Pyrenean Zone, 8 km north of the North Pyrenean Fault (Figures 1 and 2). The geologic location is the Hercynian Agly massif between two Mesozoic synclines: the Saint-Paul de Fenouillet syncline to the north and the Boucheville syncline to the south. The Agly massif is delimited on the south by the Trilla-Belesta fault considered as a ramification of the North Pyrenean Fault, and on the north by the Clue-de-la-Fou fault (Figure 2). This massif is constituted by granitic and metamorphic materials of Hercynian age. The last phase of uplift occurred during the upper Cretaceous (Delay, 1989). During the Alpine phase of the Pyrenean orogeny, the Agly massif fractured, developing strike-slip faults oriented N110 °, which were then distorted during the Oligocene (Figure 2) (Fonteilles, 1970; Delay, 1989).

Both historical and instrumental seismicity reveal that the Agly massif area is still seismically active. In particular, three earthquakes occurred in the Saint-Paul de Fenouillet area in 1920 and 1922 (Figure 1), with MSK intensities about V–VI, VI–VII, and VI respectively (Cadiot et al., 1979; Lambert and Levret-Albaret, 1996). A regional network, with a mesh of about 50 km, was established at the end of 1988 by the Observatoire Midi-Pyrénées in Toulouse and the Servei Geològic de Catalunya in Barcelona (SGC/OMP (1989–1995)). In the intervening 6 years, it has recorded several earthquakes in the Saint-Paul de Fenouillet region with a duration magnitude M_l between 1.0 and 3.4 (Figure 2).

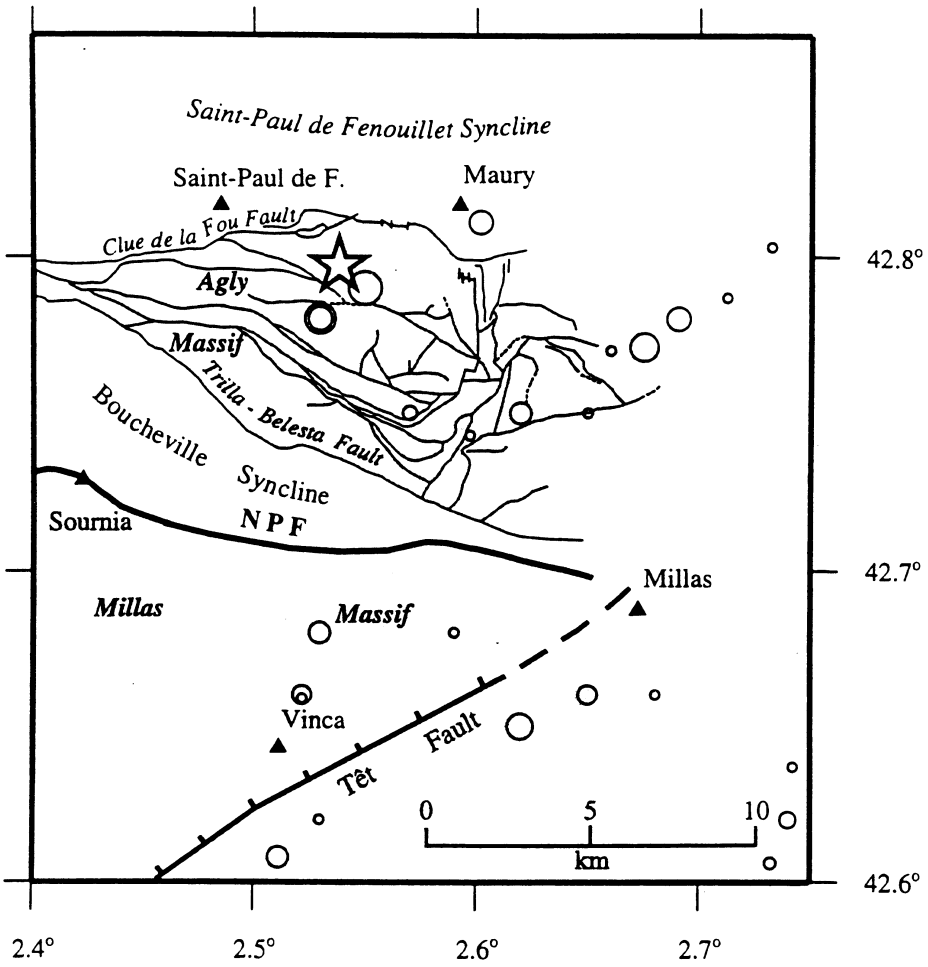

Figure 2. Tectonic map of the Agly massif redrawn from Delay (1989) and instrumental seismicity recorded by the regional seismic network installed at the end of 1988 by the Observatoire Midi-Pyrénées (Toulouse, France) and the Servei Geològic de Catalunya (Barcelona, Spain) (SGC/OMP, (1989–1995)). This seismicity covers the period from 1 January, 1989 to the 18 February, 1996 main shock (star). The symbol size is proportional to the magnitude M_l (from 1.0 to 3.4). The grey areas correspond to the Palaeozoic Massifs and the white areas to the Mesozoic basins. NPF: North Pyrenean Fault.

The nearest station of the permanent Pyrenean network (station MTHF in Figure 3) is 15 km north of St-Paul de Fenouillet, in the Mouthoumet massif (Figure 1).

In this paper, we analyse the main shock of 18 February, 1996 and the most important aftershocks in the following two months, using the data from the permanent Pyrenean seismological network, and, for the events occurring during the following two weeks, those of the temporary stations. Both hypocentre locations and focal mechanisms will bring important elements for a better understanding of the present-day tectonics of this region, a subject which was heretofore largely unknown.

The main shock (18 February, 1996)

It occurred at 1 h 45 min 45 s UT, and was felt throughout all south-western France and northern Spain, in a region of 150 km around the epicentre, including Perpignan, Carcassone, Toulouse (France) and Barcelona (Spain). Nobody was injured, but numerous masonry houses cracked. The local magnitude (M_L) was estimated at 5.6 by the LDG (Laboratoire de Détection et de Géophysique, Commissariat à l'Énergie Atomique in Paris) and by the RENASS (RÉseau NAtional de Surveillance Sismique in Strasbourg), at 5.2 by the SGC-ICC (Servei Geològic de Catalunya – Institut Cartogràfic de Catalunya in Barcelona), and at 5.0 by the IGN (Instituto Geogràfico Nacional in Madrid).

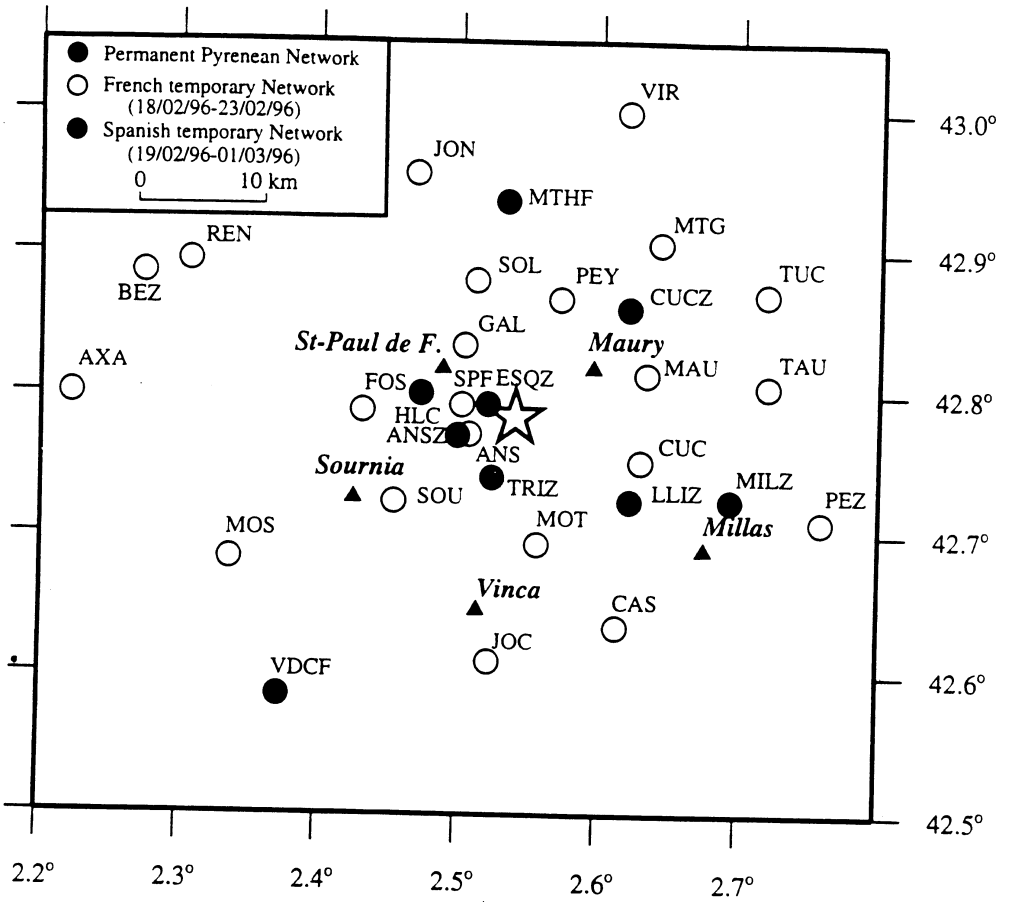

Figure 3. Temporary seismological stations installed in the Saint-Paul de Fenouillet area between 18 and 23 February, 1996. The star corresponds to the 18 February, 1996 main shock. The two permanent stations, MTHF and VDCF, are the nearest stations of the permanent Pyrenean network.

The US Geological Survey gave a body-wave magnitude m_b of 4.8. Nevertheless, no surface breaks were observed and no houses collapsed.

Some interesting hydrological phenomena were observed before and after the 'quake. In Saint-Paul de Fenouillet area there are about a dozen hot springs. The largest one, located 1.5 km south of town (the so-called Clue-de-la-Fou source, Teissier, 1994), experienced a temperature increase of several degrees after the earthquake. Several local observers claim that gas emanated from the ground as bubbles in the Agly river, beginning 15 days before the main shock. This emanation was located exactly on the Clue-de-la-Fou contact, close to the previously mentioned spring. We observed it until it stopped 5 days after the 'quake. Such hydrological phenomena have been previously observed to precede or follow other earthquakes, and are usually ascribed to a change in the local stress field (Dobrovolsky et al., 1979).

Table 1. P velocity model used for the locations of the main shock and its aftershocks, the *Vp*/*Vs* ratio used is 1.75 [*after Njike Kassala et al., 1992*].

P Velocity (km/s)	Depth (km)
5.5	0.0–1.0
5.6	1.0–4.0
6.1	4.0–11.0
6.4	11.0–34.0
8.0	>34.0

This event is the strongest one in France to be well recorded instrumentally. In addition to the Pyrenean stations (see Souriau and Granet, 1995, for description of the permanent Pyrenean seismological network), the earthquake was also recorded by regional networks in the Rhine Graben, the Alps, the Massif Central, Spain and Italy, by a total of 114 recording sites. The

Table 2. Locations of the St-Paul de Fenouillet earthquake obtained in this study and by various institutions: the RENASS (RÉseau NAtional de Surveillance Sismique, Institut de Physique du Globe de Strasbourg, France), the OMP (Observatoire Midi-Pyrénées, Toulouse, France) and the SGC (Servei Geològic de Catalunya, Barcelona, Spain), the LDG (Laboratoire de Détection et de Géophysique, Bruyères-le-Châtel, France) and the IGN (Instituto Geogràfico Nacional, Madrid, Spain).

	Latitude (N)	Longitude (E)	Depth (km)
This study	42° 47.81′	2° 32.30′	7.70
RENASS	42° 48.00′	2° 33.00′	6.00
OMP-SGC	42° 48.00′	2° 31.80′	8.00
LDG	42° 48.00′	2° 30.00′	11.00
IGN	42° 48.70′	2° 33.90′	11.00

hypocentral location was computed with the Hypo71 code (Lee and Lahr, 1975) using the P- and S-wave arrival times. The P velocity model used is a multilayer model (Table 1) determined from seismic profiles (Gallart et al., 1981; Daignières et al., 1982). The V_p/V_s ratio of 1.75 has been determined using the Wadati method, from 15 years of regional seismicity (Njike Kassala et al., 1992). For the determination of the hypocentre, we excluded stations at distances greater than 120 km for two reasons. First is the heterogeneity of the crust in France and Northern Spain. The Pyrenean velocity model is not valid for paths to the Alps, the Massif Central and the Rhine Graben. Moreover, the Moho jump across the North Pyrenean Fault would be difficult to handle in a location computation including the refracted arrivals. Another reason is that the Pn phase (the P-wave refracted on the Moho discontinuity) becomes the first arrival at this distance of 120 km. Because the Hypo71 code does not distinguish between direct and refracted arrivals, we restrict our data set to the direct P-wave arrivals. This restriction improves the confidence of the estimated parameters, particularly the focal depth. Consequently, only 20 stations were retained among 114. This is sufficient for computing an accurate location because the main shock is near the permanent Pyrenean stations.

The location obtained for the main shock is latitude N 42° 47.81′ and longitude E 2° 32.30′ with a depth of about 7.7 km (Figure 2). The uncertainties are about ± 1.5 km for the epicentral position and ± 2.5 km for the focal depth. Table 2 compares our determination to the different locations estimated by other institutions immediately after the quake. Except for the location given by IGN, which had direct access only to a smaller number of records, the various determinations are consistent. The most poorly determined parameter is the focal depth. This is a typical problem when no records are available close to the epicentre. Our determination of the focal depth should be the best, because the nearest station to the hypocenter (MTHF at 17 km, Figure 3) is part of the permanent Pyrenean seismological network.

The focal mechanism was determined using the P-wave first motions at 82 stations having clear P polarities. The focal sphere obtained is shown in Figures 4 and 5 and the fault plane parameters are given in Table 4. This mechanism is very well constrained: the uncertainties on the strike and dip for both nodal planes are about ± 5 °. The fault plane solution shows an E–W striking subvertical nodal plane and a N–S striking nodal plane dipping west at 58 °. We chose the E–W striking nodal plane as the fault plane because of the east-west trends in the local geologic structures: the Saint-Paul de Fenouillet syncline, the Clue-de-la-Fou fault and the major faults in the Agly massif (Figure 2). Moreover, the instrumental seismicity recorded for the period 1963–87 by the LDG/CEA, although fairly inaccurate in this region, reveals an E–W trend of the epicentre distribution in this area, about 10–15 km north of the North Pyrenean Fault. In addition, there is no geologic evidence for N–S striking tectonic structures in the Agly massif corresponding to the other nodal plane. Thus, the mechanism of the rupture is almost unambiguously an E–W, left-lateral strike-slip fault inside the Agly massif.

The aftershocks

Within 24 hours of the main shock, we installed a temporary network in the area around the epicentre (Figure 3). The network included 9 one-component stations and 16 three-component stations for the French team, and 5 three-component stations for the Spanish team. The French stations remained in the field until 23 February, 1996 and the Spanish stations until March 1, 1996. Approximately 500 events were recorded. We present here only the 37 events with magnitude M_l greater than 1.8, occurring during the two months after the main shock. This data set comprises the complete earthquake sequence recorded by the permanent network. We used the data of the temporary network, when available, to estimate the locations and the focal mechanisms.

The locations were computed with the same method and the same velocity model as the main shock. The

Table 3. Aftershock locations. M_l: Duration magnitude determined on the Pyrenean station MLSF (Moulis); M_L: local magnitude determined by RENASS in Strasbourg that is always overestimated. (a): events located from the permanent Pyrenean seismological network only; (b): events located from the permanent Pyrenean seismological network and the temporary network. See text for discussion.

Date yymmdd	Origin Time hh:mm:ss	Lat. (N)	Long. (E)	Depth(km)	M_l	M_L	
960218	01:54:34.1	42°44.47′	2°31.82′	4.2	2.3		(a)
960218	02:02:32.5	42°47.17′	2°32.19′	10.6	3.2	3.7	(a)
960218	02:27:02.4	42°46.28′	2°31.19′	9.7	3.4	4.0	(a)
960218	02:38:40.0	42°47.18′	2°32.54′	4.3	2.3	2.7	(a)
960218	04:28:56.5	42°46.68′	2°32.50′	1.9	3.0	3.2	(a)
960218	04:37:19.1	42°46.66′	2°32.10′	4.2	1.8		(a)
960218	09:17:08.4	42°46.99′	2°31.77′	3.9	2.7	3.0	(a)
960218	15:57:55.9	42°46.89′	2°31.60′	3.8	3.1	3.3	(a)
960219	01:38:56.3	42°46.19′	2°31.57′	6.2	2.9	3.0	(b)
960219	03:13:08.7	42°44.13′	2°31.73′	3.4	2.0	2.6	(b)
960219	03:40:52.2	42°45.57′	2°31.64′	7.9	3.1	2.9	(b)
960219	04:25:01.1	42°46.18′	2°31.74′	7.0	3.3	3.8	(b)
960219	13:10:51.9	42°47.14′	2°35.72′	5.3	1.9		(b)
960219	16:04:23.1	42°47.28′	2°33.45′	8.8	1.9		(b)
960219	20:25:18.0	42°48.78′	2°35.11′	10.6	1.8		(b)
960219	22:14:32.3	42°47.74′	2°35.12′	8.3	1.8		(b)
960220	09:22:23.2	42°46.69′	2°31.90′	11.0	2.0		(b)
960220	12:58:30.3	42°46.70′	2°31.84′	7.2	3.2	3.6	(b)
960222	07:07:32.1	42°46.94′	2°32.18′	6.7	1.9	2.4	(b)
960223	00:06:33.0	42°47.14′	2°31.12′	8.6	1.8	2.3	(b)
960225	07:23:49.3	42°46.14′	2°32.51′	5.9	2.3	2.8	(b)
960226	18:01:18.7	42°46.67′	2°31.53′	6.2	2.0	2.4	(b)
960227	02:18:12.8	42°47.09′	2°31.62′	4.3	1.8	2.3	(b)
960227	21:31:21.2	42°45.54′	2°32.79′	3.6	2.1	2.5	(b)
960227	23:08:55.3	42°46.49′	2°33.53′	4.7	1.8	2.3	(b)
960228	00:41:21.8	42°46.52′	2°32.28′	6.0	1.8	2.3	(b)
960228	04:31:30.8	42°46.87′	2°33.54′	4.6	2.3	2.6	(b)
960229	02:28:12.8	42°46.73′	2°31.72′	6.5	2.0	2.5	(b)
960301	07:32:38.4	42°47.16′	2°31.27′	7.0	2.0	2.5	(b)
960304	13:19:31.2	42°46.62′	2°32.20′	1.8	3.0	3.3	(a)
960313	04:39:57.1	42°47.01′	2°32.13′	2.8	3.0	3.2	(a)
960315	21:39:10.8	42°45.14′	2°31.44′	6.5	2.2	2.9	(a)
960328	08:04:30.5	42°46.56′	2°32.31′	4.0	3.1	3.4	(a)
960330	18:37:30.6	42°46.81′	2°33.08′	1.0	3.3	3.2	(a)
960404	05:57:48.0	42°47.28′	2°33.09′	3.7	3.1	3.3	(a)
960416	15:54:49.0	42°47.31′	2°33.29′	5.0	2.6		(a)
960420	03:54:55.9	42°47.01′	2°31.30′	0.4	2.3	2.8	(a)

results of the locations are given in Table 3 and in Figure 4. In this data set, there are two subsets of events: those recorded by only the permanent network because the temporary network was not yet installed or was dismantled (events labelled (a) in Table 3), and those recorded by both networks (events labelled (b) in Table 3). Consequently, the uncertainties in location are not the same for the two sets of events. To determine these uncertainties, we computed the location of all events without the temporary stations, and thus estimate any biases inherent to the use of the large-scale permanent network. From this test, we estimated that

Table 4. Fault plane solution parameters of the main shock (bold) and of the 8 aftershocks shown in Figure 4.

Date yymmdd	Time hh:mm	Strike 1 degrees	Dip 1 degrees	Rake 1 degrees	Strike 2 degrees	Dip 2 degrees	Rake 2 degrees
960218	**01:45**	**96**	**84**	**−43**	**192**	**47**	**−171**
960218	02:02	53	43	24	305	74	130
960218	02:27	116	69	102	266	24	62
960219	01:38	350	10	120	140	81	85
960219	04:25	287	80	174	18	84	10
960220	09:22	286	55	87	111	35	94
960220	12:58	345	44	−47	113	59	−123
960223	00:06	270	40	105	71	52	78
960225	07:23	74	32	102	240	59	83

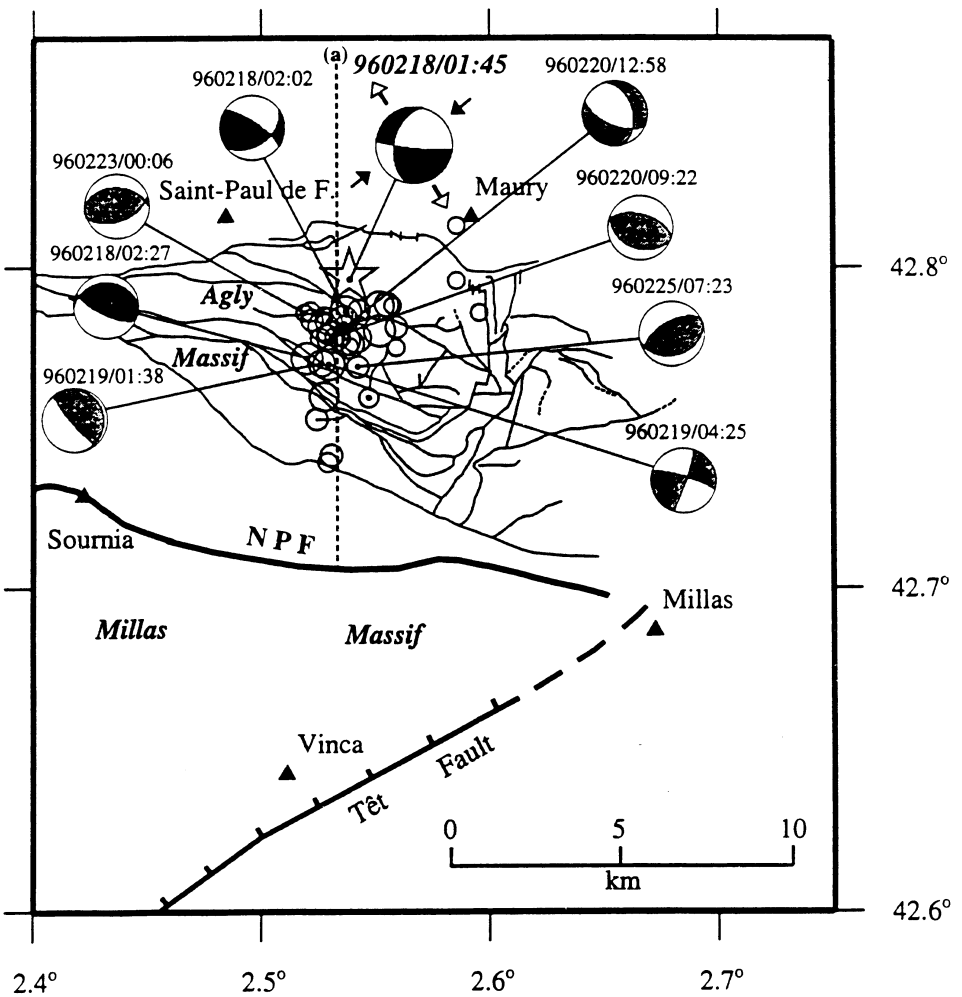

Figure 4. Epicentral locations and fault plane solutions (lower hemisphere) of the 18 February, 1996 main shock and of the aftershocks. The locations are given for the 37 aftershocks of magnitude of duration M_l above 1.8. The shaded fault plane solutions are determined with at least one P polarity of the temporary stations and the black fault plane solutions are determined without data from the temporary network, not yet installed. (a) Trace of the cross-section shown on Figure 6. Compressional (P-) and extensional (T-) axes for the main shock are shown as black and white arrows respectively.

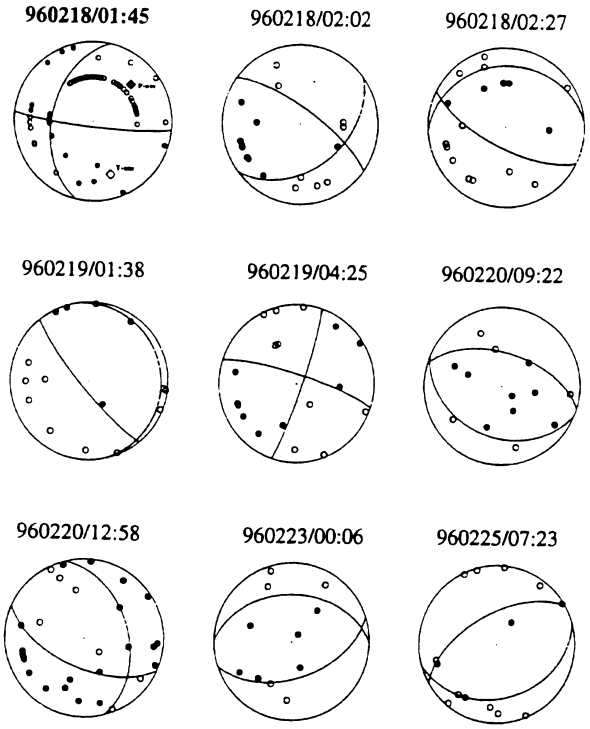

Figure 5. Fault plane solutions of the 18 February 1996 earthquake in Saint-Paul de Fenouillet, obtained with 82 P first motions from various regional networks in Europe and of the 8 main aftershocks. Polarities of P-waves are plotted on the lower equal-area hemisphere of the focal sphere, with black circles for compressive arrivals and open circles for dilatational arrivals.

the mean uncertainties for the locations with data from the permanent network are (events (a) in Table 3) only ± 2.8 km and ± 3.5 km for the epicentral position and the depth respectively; whereas the uncertainties for the events located with both networks are ± 1.1 km and ± 1.5 km for the epicentral position and the depth respectively. Finally, the mean travel time residual for the location with both networks and for the all events is 0.31 ± 0.06 s. We note that most of the aftershocks are located immediately south of the main shock, defining a cluster in the centre of the Agly massif (a 8 km × 8 km area, Figure 4). Moreover, some aftershocks located with only the permanent network reach the southern limit of the Agly massif on the Trilla-Belesta Fault. These events occurred within the first day after the main shock and then eliminate a north-south propagation of the deformation in the Agly massif.

We determined 8 focal mechanisms using the P first motions for the events with sufficient magnitude (Figures 4 and 5, Table 4). The uncertainties of the nodal planes in strike and dip are typically ± 15 ° except for the mechanism of the 960219/01:38 event, for which the uncertainties for the strikes of the nodal planes is ± 25 °. We distinguished in Figure 4 the mechanisms determined with at least one P polarity of the temporary stations (shaded fault plane solutions) from those (black fault solutions) determined without data from the temporary network not yet installed. Mechanisms are reverse faults striking approximately N110° (six of eight). The other two events include one strike-slip mechanism and one normal faulting mechanism. Nevertheless, the E–W striking nodal planes align with the major faults observed in the Agly massif.

Figure 6 projects all aftershock locations and fault plane solutions on a vertical N–S cross-section (plotted (a) in Figure 4) superimposed on a simplified geologic cross-section. The depths of the aftershocks range fairly uniformly between 0 and 11 km (see also Table 3). The aftershocks are spatially distributed inside the Agly massif. For this reason, and considering the interpretations from the ECORS profile (Gallart et al., 1981; Daignières et al., 1982; Choukroune and ECORS Team, 1989; Choukroune, 1992), the deepest events can be interpreted as the lower limit of the Agly massif and, in any case, as the lower limit of the brittle upper crust.

Discussion and conclusion

The magnitude $M_L = 5.2$ Saint-Paul de Fenouillet earthquake is the first important earthquake to be well recorded instrumentally in the Pyrenees. Using all the records of permanent networks, we have determined accurately the earthquake location and its fault plane solution. With the additional data from a temporary network of 30 portable seismological stations, we located the 37 main aftershocks ($M_l > 1.8$) occurring during the two-month crisis following the main event, and determined focal mechanisms for 8 of them (Figures 4 and 6). The analysis reveals that the main shock is not located on the senestral North Pyrenean Fault, which corresponds to the east-west suture between the Iberian and Eurasian plates, but 8 km northward, inside the highly fractured Agly massif. The fault plane solution is an E–W left-lateral strike-slip fault with a small, normal faulting component.

Aftershocks of significant magnitudes M_l (1.8 to 3.4) occurred during a period of two months following the main shock. Most of them are in a cluster immediately south of the main shock (Figure 4), with depths varying from 0 to 11 km. The location of these aftershocks may indicate that the fault activated by the main

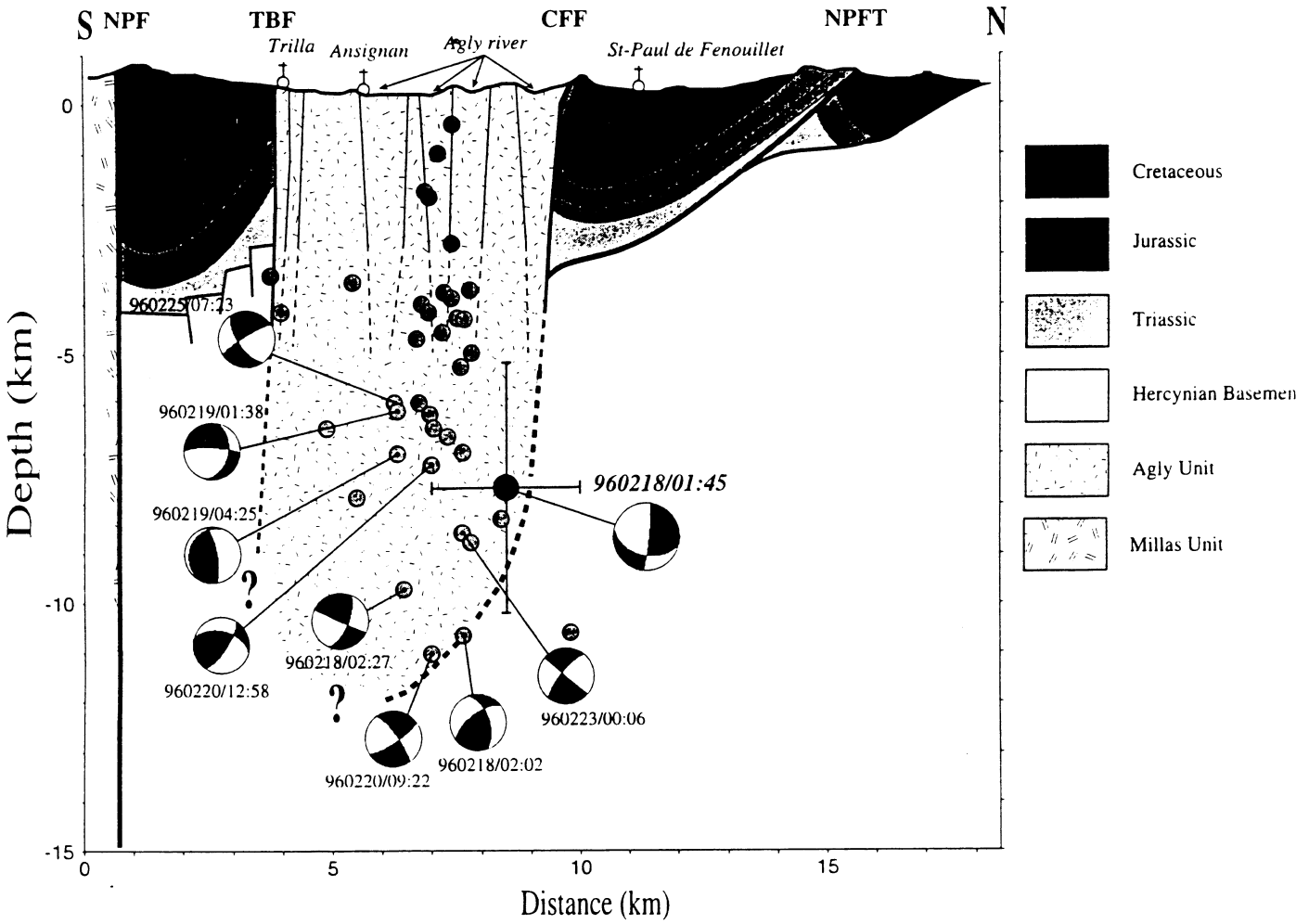

Figure 6. North-South cross-section with no vertical exaggeration across the Agly massif (profile (a) in Figure 4). All hypocentres and fault plane solutions are projected on to the vertical plane. Symbol with the location error bars is the main shock. NPF: North Pyrenean Fault; TBF: Trilla-Belesta Fault; CFF: Clue-de-la-Fou Fault; NPFT: North Pyrenean Frontal Thrust.

shock is inside the Agly massif. According to the scaling laws (Kanamori and Anderson, 1975), a magnitude $M_l = 5.2$ earthquake needs a rupture plane of approximately 25 km^2 (5 km × 5 km). Such a vertical fault plane with an E–W orientation, crossing the aftershock cluster and within the uncertainties of the main shock location, exists in the Agly massif (Figure 4).

The fault plane solutions determined for eight aftershocks indicate a predominant reverse faulting mechanism with a WNW-ESE orientation, which is consistent with the orientations of the faults observed in the Agly massif (Delay, 1989; Philip et al., 1992). Some neotectonic observations (Philip et al., 1992) have shown reverse faults with a left-lateral component in the Agly massif. The mechanism of the main shock is consistent with this left-lateral component but not with the reverse component. In contrast, however, the fault plane solutions of the aftershocks are reverse faulting with mostly right-lateral component (Figure 4). We infer that the faulting in the Agly massif must be complex, and that the main shock reactivated or triggered several small faults or fractures. Nevertheless, the N–S trend of the averaged aftershocks P-axes denotes northward overthrusting inside the Agly massif, consistent with the general north-south shortening of the Pyrenees, well observed in the North Pyrenean Zone (Choukroune and Mattauer, 1978; Légier et al., 1987; Delay, 1989; Choukroune, 1992).

The Agly area has been recognised as an active area from both historical and instrumental seismicity. The instrumental seismicity of the last 35 years does not indicate any activity along the North Pyrenean Fault in this area, but a 1981 earthquake, located 50 km west of Saint-Paul de Fenouillet on the North Pyrenean Fault,

exhibits the same focal mechanism and the same P and T axes as the 1996 event (Olivera et al., 1996). Although it is premature to draw a conclusion from a single event, the present result would suggest that the North Pyrenean Fault seems to be relayed northward by a complex fault system.

Another possibility is to consider that the deformation occurs inside a ~15 km wide, E–W, senestral shear zone, bounded to the north by the Saint-Paul de Fenouillet basin or by the North Pyrenean Frontal Thrust, and to the south by the North Pyrenean Fault. A senestral shear deformation in the Saint-Paul de Fenouillet syncline is indeed revealed by the presence of a few small faults en echelon west of Saint-Paul de Fenouillet town, and by a few secondary folds with vertical axial planes consistent with an E-W shear (D. Leblanc, personal communication).

In both cases, the main tectonic signature is present-day senestral motion in the eastern part of the Pyrenees. This left-lateral movement is more or less accepted in the different geodynamic models for the Pyrenean range. Moreover, the Catalan earthquakes (Olivera et al., 1996), the Arette microseismicity (Gagnepain-Beyneix, 1987) and the Arudy earthquake with some of its aftershocks (Gagnepain-Beyneix et al., 1982) exhibit right-lateral strike-slip on E–W striking faults and P axes at N160–170° on average. Consequently, the eastern part of the French Pyrenees clearly has a different tectonic regime than the rest of the range. Such a separate regime seems more related to the regional stress field in the Alps than the Pyrenean range. Indeed, the P axes in the Languedoc and Provence regions have the same orientation as the Saint-Paul de Fenouillet event (Wehile et al., 1997).

Another point which calls for comment is the depth of the foci. The main shock depth (~8 km) indicates that the Agly massif is deeply rooted in the north Pyrenean sediments. This could indicate that the Agly massif does not have an allochton origin, as proposed for the North Pyrenean Massifs (Goldberg et al., 1986; Souquet and Peybernès, 1987). On the other hand, aftershocks are observed down to 11 km, indicating that the fractures which affect the Agly massif extend at least down to this depth which also corresponds to a significant change of the P velocities (Gallart et al., 1980). Crustal events at greater depth are in any case uncommon, as this depth corresponds to the overall limit between the brittle upper crust and the ductile lower crust. This hypothesis has a direct consequence for the geometry of the faults at depth, as shown in Figure 6: The North Pyrenean Frontal Thrust (N.P.F.T., Figure 6) dipping to the south, connects at depth to the North Pyrenean Fault, forming a ramp at 10–12 km depth beneath the Agly massif and the Clue-de-la-Fou Fault (CFF, Figure 6), connecting at 4–5 km depth to this ramp. This deep feature is consistent with the crustal scale cross-sections inferred from the interpretations of the Pyrenean ECORS seismic profile (Daignières et al., 1982; Roure et al., 1989; Choukroune, 1992).

The 1996 Saint-Paul de Fenouillet earthquake sequence occurred in a rather well known geological context. Our analysis has shown that the active fault is not the suture of two plates as might be expected, but a more northern fault inside the Agly massif. Important new elements concern the width of the deformed zone, the geometry of the faults and the depth of the structure involved. A careful analysis of the hundreds of small events recorded during the first week after the main shock will probably reveal a refined image of the faulted structures and of the stress release pattern in the Agly region.

Acknowledgments

We are grateful to those who helped us during the field work: G. Barruol, D. Beaumont, H. Blumentritt, J. M. Douchain, A. Herrero, R. Russo, J. Sahr and M. Sylvander. We thank H. Dufumier and the MedNet staff for rapidly providing the Italian data. The Consejo Superior de Investigaciones Cientificas (CSIC), the Universitat de Barcelona (UB) and the Institut Cartogràfic de Catalunya (ICC) provided instruments. We also thank M. Blanc, D. Hatzfeld, G. Poupinet, J. C. Olmedillas, J. Casas, J. Diaz, J. Gallart, M. Granet, the Mayor B. Foulquier and the Mayor's office in Saint-Paul de Fenouillet, and the RENASS for their precious logistic support, as well as M. Mattauer, J. L. Bouchez, D. Leblanc and M. de Saint Blanquat for helpful discussions, P. Bernard and two other anonymous referees for their constructive criticism of the manuscript. This work was supported by grants from the French Institut National des Sciences de l'Univers (CNRS/INSU).

References

Bouhallier, H., Choukroune, P. and Ballèvre, M., 1991, Évolution structurale de la croûte profonde Hercynienne: exemple du massif de l'Agly (Pyrénées Orientales, France), *C. R. acad. Sci. Paris* **312**, 647–654.

Briais, A., Armijo, R., Winter, T., Tapponnier, P. and Hebbecq, A., 1990, Morphological evidence for Quaternary normal faulting

and seismic hazard in the Eastern Pyrenees, *Annales Tectonicae*, vol. IV, **1**, 19–42.

Cadiot, B., Delaunay, J. and Vogt, J., 1979, Tableaux anthologiques de la sismicité de la France, in Vogt, (ed.), *Les Tremblements de terre en France, Éditions du Bureau de Recherche Géologiques et Minières* **96**, 17–152.

Choukroune, P., 1992, Tectonic evolution of the Pyrenees, *Annu. Rev. Earth Planet. Lett.* **20**, 143–158.

Choukroune, P. and ECORS Team, 1989, The ECORS Pyrenean deep seismic profile reflection data and the overall structure of an orogenic belt, *Tectonics* **8**, 23–29.

Choukroune, P. and Mattauer, M., 1978, Tectonique des plaques et Pyrénées: sur le fonctionnement de la faille transformante Nord-Pyrénéenne; comparaison avec les modèles actuels, *Bull. Soc. Géol. France* **20**, 689–700.

Daignières, M., Gallart, J., Banda, E. and Hirn, A., 1982, Implications of the seismic structure for the orogenic evolution of the Pyrenees range, *Earth Planet. Sci. Lett.* **57**, 88–100.

Daignières, M., de Cabissole, B., Gallart, J., Hirn, A., Surinach, E. and Torné, M., 1989, Geophysical constraints on the deep structure along the ECORS Pyrenees line, *Tectonics* **8**, 1051–1058.

Delay, F., 1989, Le massif Nord-Pyrénéen de l'Agly (Pyrénées Orientales). Évolution tectono-métamorphique et exemple d'un amincissement crustal polyphasé, *Thèse de Doctorat*, Université de Lille, France.

Dobrovolsky, I. P., Zubkov, S. I. and Miachkim, V. I., 1979, Estimation of the size of earthquake preparation zones, *Pageoph.* **117**, 1025–1044.

ECORS Pyrenees Team, 1988, The deep reflection seismic survey across the Pyrenees, *Nature* **331**, 508–511.

Engeser, T. and Schwentke, W., 1986, Towards a new concept of the tectonogenesis of the Pyrenees, *Tectonophysics* **129**, 233–242.

Fonteilles, M., 1970, Géologie des terrains métamorphiques du massif hercynien de l'Agly (Pyrénées Orientales), *Bull. Bureau de Recherche Géologiques et Minières* **4**, 21–72.

Gagnepain-Beyneix, J., Haessler, H. and Modiano, T., 1982, The pyrenean earthquake of 29 February, 1980: an example of complex faulting, *Tectonophysics* **85**, 273–290.

Gagnepain-Beyneix, J., 1987, Étude expérimentale des tremblements de terre. Exemple de la région d'Arette (France), *Thèse de Doctorat*, Université Paris VII, France.

Gallart, J., Daignières, M., Banda, E., Surinach, E. and Hirn, A., 1980, The Eastern Pyrenean domain: lateral variations at crustal-mantle level, *Ann. Geophys.* **36**, 141–158.

Gallart, J., Banda, E. and Daignières, M., 1981, Crustal structure of the Paleozoic Axial Zone of the Pyrenees and transition to the North Pyrenean Zone, *Ann. Geophys.* **37**, 457–480.

Gallart, J., Olivera, C., Daignières, M. and Hirn, A., 1982, Quelques données récentes sur la relation entre fractures crustales et séismes dans les Pyrénées Orientales, *Bull. Soc. Géol.* France **24**, 293–298.

Goldberg, J. M., Maluski, H. and Leyreloup, A. F., 1986, Petrological and age relationship between emplacement of magmatic breccia, alkaline magmatism, and static metamorphism in the north pyrenean zone, *Tectonophysics* **129**, 275–290.

Hirn, A., Daignières, M., Gallart, J. and Vadell, M., 1980, Explosion seismic sounding of throws and dips in the continental moho, *Geophys. Res. Lett.* **7**, 263–266.

Kanamori, H. and Anderson, D. L., 1975, Theoretical basis of some empirical relations in seismology, *Bull. Soc. Seism. Am.* **65**, 1073–1085.

Lambert, J. and Levret-Albaret, A., 1996, Mille ans de séismes en France, *Ouest Éditions – Bureau de Recherches Géologiques et Minières – Électricité de France – Institut de Protection et de Sureté Nucléaire*, 80 pp.

Lee, W. H. K. and Lahr, J. C., 1975, HYPO71 (revised): a computer program for determining hypocenter, magnitude and first motion pattern of local earthquakes, *U.S. Geol. Survey Open-File report* **75–311**, 116 pp.

Légier, C., Tempier, C. and Vauchez, A., 1987, Tectonique tangentielle ductile syn-métamorphe d'âge crétacé supérieur dans la couverture du massif de l'Agly (zone Nord-Pyrénéenne Orientale), *C. R. acad. Sci.* Paris **305**, 907–911.

Mattauer, M., 1990, Une autre interprétation du profil ECORS Pyrénées, *Bull. Soc. Géol. France* **6**, 307–311.

Njike Kassala, J. D., Souriau, A., Gagnepain-Beyneix, J., Martel L. and Vadell, M., 1992, Frequency-magnitude relationship and Poisson's ratio in the Pyrenees, in relation to earthquake distribution, *Tectonophysics* **215** , 363–369.

Olivera, C., Susagna, T., Fleta, J., Figueras, S., Goula, X., Roca, A., Martel, L., Souriau, A. and Grellet, B., 1996, Tectonic implications of the $M > 4$ earthquakes occurred in Catalonia-Eastern Pyrenees area in the period 1990–1996, *Proceedings of the XXV European Seismological Commission General Assembly*, Reykjavik, Iceland.

Paquet, J. and Mansy, J. L., 1991, La structure de l'Est des Pyrénées (transversale du massif de l'Agly): un exemple d'amincissement crustal, *C. R. acad. Sci. Paris* **312**, 913–919.

Philip, H., Bousquet, J. C., Escuer, J., Fleta, J., Goula, X. and Grellet, B., 1992, Présence de failles inverses d'âge quaternaire dans l'Est des Pyrénées: implications sismotectoniques, *C. R. acad. Sci. Paris* **314**, 1239–1245.

Puigdefabregas, C. and Souquet, P., 1986, Tecto-sedimentary cycles and depositional sequences of the Mesozoic and Tertiary from the Pyrenees, *Tectonophysics* **129**, 173–203.

Rehaut, J. P., Boillot, B. and Mauffret, A., 1984, The Western Mediterranean Basin geological evolution, *Mar. Geol* **55**, 447–477.

Roure, F., Choukroune, P., Berastegui, X., Munoz, J. A., Villien, A. and ECORS working group, 1989, ECORS deep seismic data and balanced cross-sections: geometric constraints on the evolution of the Pyrenees, *Tectonics* **8**, 41–50.

SGC/OMP (1989–1995), Seismic Activity in the Pyrenees. *Servei Geològic de Catalunya and Observatoire Midi-Pyrénées de Toulouse*.

Souquet, P. and Peybernès, B., 1987, Allochtonie des Massifs primaires Nord-pyrénéens des Pyrénées centrales, *C. R. acad. Sc. Paris* **305**, 733–739.

Souriau, A. and Granet, M., 1995, A tomographic study of the lithosphere beneath the Pyrenees from local and teleseismic data, *J. Geophys. Res.* **100**, 18117–18134.

Teissier, J. L., 1994, Projet de réhabilitation des captages en vue de la création d'une unité d'embouteillage d'eau minérale – Étude hydrogéologique préalable aux travaux de réhabilitation, *Bureau de Recherches Géologiques et Minières*, Report 1470, 50 pp.

Torné, M., de Cabissole, B., Bayer, R., Casas, A., Daignières, M. and Rivero, A., 1989, Gravity constraints on the deep structure of the Pyrenean belt along the ECORS profile, *Tectonophysics* **165**, 105–116.

Vielzeuf, D. and Kornprobst, J., 1984, Crustal splitting and the emplacement of the Pyrenean lherzolites and granulites, *Earth Planet. Sci. Lett.* **67**, 87–96.

Wehrle, V., Müller, B. and Fuchs, K., 1997, Short scale variations of tectonic regimes in the western european stress province, Terra Nova, Abstract suppl. n. 1, 9, 310.